The International Journal of Advanced Manufacturing Technology (2022) 121:753–763
https://doi.org/10.1007/s00170-022-09336-4

ORIGINAL ARTICLE

Shape and position design of two-step micro-channel on plate during rubber pad forming process based on simulation

Fei Teng[1] · Hongyu Wang[1] · Shengnan Shi[1] · Jirui Li[1] · Juncai Sun[1] · Jie Sun[2] · Shunhu Zhang[3]

Received: 22 April 2021 / Accepted: 7 May 2022 / Published online: 20 May 2022

Abstract

Rubber pad forming is an advanced processing technology to form the metal sheet. The micro-channel on the plate can be formed by both rubber pad and the metal mold. With the development of micro-channel, a two-step micro-channel has been applied in more and more fields such as fuel cell bipolar plate. However, little attention was given to the forming strategy for these unique channels. In this paper, the rubber pad forming process is used to form the entire SS304 sheet with two-step channels. In order to design the micro-channel structure with good formability, the main parameters of the two-step micro-channel are discussed through finite element modeling (FEM) and forming experiment. Not only for the geometric parameters for structures like length, width, edge chamfer, and the height ratio of first to second step, but also for the spatial distribution like the number and distance of two-step micro-channels in the entire plate. In addition, MATLAB is used to study the influences on the final forming results because of the various parameters. And then, the plates can be precisely formed when the structure is suitable, while micro-channels with unsuitable structure cannot be formed as designed. Finally, based on the FEM and forming experiment results, a design strategy is provided in the conclusions.

Keywords Finite element method · Two-step micro-channel · Rubber pad forming · Forming experiment

Abbreviations

D_1, D_2	Edge chamfer
H_1:H_2	Height ratio of first to second step
O	The original point of the coordinate system
l_1	Length of the plate
w_1	Width of the plate
w_2	Width of the channel
d_1	The distance between two channels
d_2	The distance between the outermost channel and the edge of the plate
n_1	The number of channels in the x-axis
n_2	The number of second-step structures
l_2	Length of the second-step structure
l_3	Length of the straight channel
d_3	The distance between second-step structures
d_4	The distance between the second-step structures and the corner area

✉ Hongyu Wang
wanghongyusci@yeah.net

[1] Transportation Engineering College, Dalian Maritime University, Dalian, Liaoning, People's Republic of China 106026

[2] State Key Laboratory of Rolling and Automation, Northeastern University, Shenyang, Liaoning, People's Republic of China 110000

[3] Shagang School of Iron and Steel, Soochow University, Suzhou, People's Republic of China 215002

1 Introduction

Rubber pad forming is a new forming process with only a few years of history. Brownie and Battikha [1] as well as Belhassen et al. [2] proposed that aluminum plates could be formed into the designed shapes through the cooperation of rubber and metal mold, because only elastic deformation was produced on rubber. Rubber can be used repeatedly. At the same time, the steel mold on one side was replaced by rubber. Forming cost was reduced greatly. In the research of Peng et al. [3, 4] and Chen and Ye [5, 6], polyurethane and punch were used to process micro-channels on thin plates. Thiruvarudchelvan [7] reviewed several rubber pad–forming technologies and found that polyurethane played an important role in the forming process. As it is shown in Fig. 1, not only polyurethane, stainless steel 304 is also used in the study of Chen et al. [8]. Since Wang et al. [9] found the formability of convex mold was much better than that of a

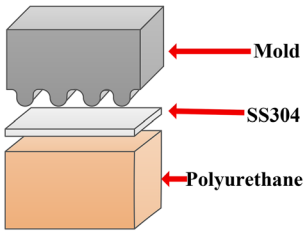

Fig. 1 Schematic diagram of rubber pad forming

concave one, polyurethane is chosen to replace the concave mold in much more researches.

As shown in Fig. 2, micro-channels are mainly used to guide fluids. And then, industrial and livelihood applications such as heat dissipation [10], gas reaction [11, 12], and drag reduction [13] are developed. Micro-channels are also widely used in the bipolar plates of PEMFC (proton exchange membrane fuel cell) because the gas flow mode is directly determined by micro-channels [3, 4]. However, it should be clear that the guiding of fluids by micro-channels should be divided into two categories. One is the horizontal direction; it is mainly based on the corner channel and the spatial distribution of straight channel. The other one is the vertical direction, which mainly depends on a three-dimensional two-step micro-channel.

As it is recorded above, many scholars have studied the process of forming micro-channel by rubber pad forming [14] on the horizontal direction. As shown in Fig. 3a, a serpentine micro-channel was researched by Ghadikolaee et al. [15] and Wang et al. [16]. Based on the reciprocating of the gas, the reaction efficiency of these micro-channels was significantly improved. In Fig. 3b, two concentric spiral micro-channels were proposed by Juarez-Robles et al. [17]. From Fig. 3c, a new flow field design in horizontal direction was proposed based on the same design concept.

However, the flows fields shown above are not changed in vertical direction. Yang et al. [18] proposed a two-step micro-channel. Based on the cyclic variation of the height and depth in the micro-channel, the fluid was forced to flow in three dimensions. This kind of micro-channel was also studied by Li et al. [19] based on finite element simulation. The forced convection of gas is more obvious in this channel. Based on this advantage, the gas reactivity and performance of PEMFC are also significantly enhanced when two-step micro-channels are applied to bipolar plates. In this paper, the two-step micro-channel is applied to the new flow field as shown in the Fig. 3c, and the structural optimization is promoted so that it can be precisely formed by the rubber pad forming process.

The forming processes of the single two-step straight channel and single corner channel were studied by the authors, respectively [9, 20]. They found that the geometries of both straight and corner channel had particularly significant effects on formability. When the parameters are suitable, the micro-channels can be well formed. This kind of Taguchi method can be used to improve product quality through design and has the advantage of low cost [21]. Teng et al. conducted a mechanical theoretical analysis of this process, but there was less discussion on the specific parameters [22]. It is worth mentioning that only structural units like second-step structure and corner channel have been studied so far. The forming process of an entire plate is still unknown. In this paper, Taguchi method was used to optimize the process parameters of rubber pad forming, and the structure with good formability was designed. Since the design of entire plate should contain both structures and spatial distribution, a study focused on completed channels is studied in this paper.

1. Firstly, the geometric parameters of second-step structure like the length, width, height ratio, and edge chamfer are studied, and these parameters have main effects on the final shapes of second-step structures.
2. Secondly, the spatial distribution of second-step structures like the number and distance of second-step structures is also discussed; also, these parameters influence the final positions of second-step structures a lot.

Based on these parameters, different molds are manufactured. In the rubber pad–forming process, the plates are

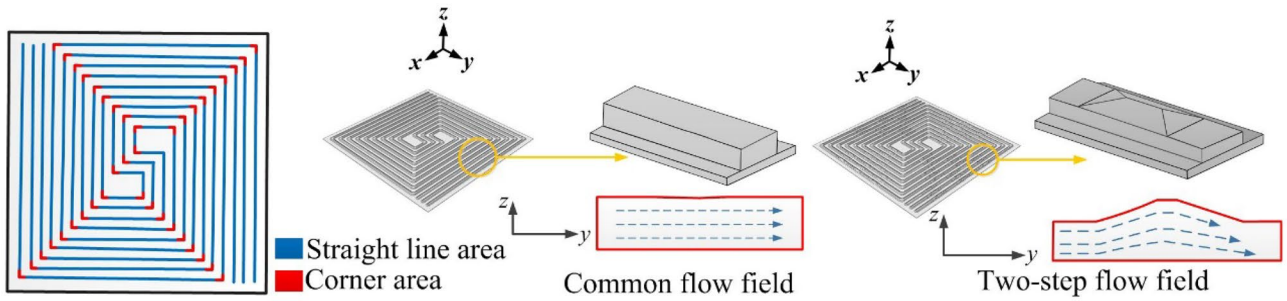

Fig. 2 Common micro-channel and two-step micro-channel

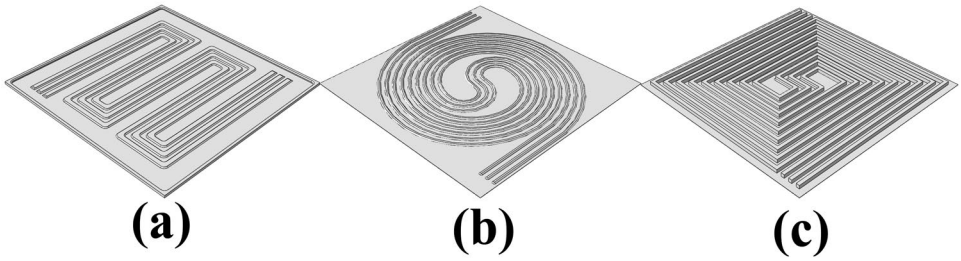

Fig. 3 Schematic diagrams of the flow fields, (**a**) serpentine micro-channel; (**b**) two concentric spiral micro-channel; (**c**) new flow field design

formed through these molds. Finite element simulations and pressing experiment are established to study this process. Flow fields with different parameters are compared based on their forming results and stress patterns. Finally, a well-formed design strategy can be obtained.

2 Modeling

In this paper, ABAQUS6.14.3 is used to simulate the whole forming process. In order to ensure the accuracy of the simulation, the rubber pad forming model of the whole plate is established. As shown in Fig. 4, the geometric parameters of molds are shown.

In order to obtain a comprehensive understanding on forming of two-step micro-channel with different shapes based on rubber pad forming, there are 11 groups with different geometric parameters. The fillet of all molds is 0.3 mm. Molds are discussed separately based on their types. As shown in Table 1, the details of parameters are displayed.

When the width of the micro channel is too small, the formability of the channel will be decreased. If the width is too large, other parameters can also be affected. Moreover, when the number of channels is increased, the distance between the channels will be decreased, which will also lead to poor formability. Therefore, it is very important to find the balance between the width and spacing of micro-channels. The best parameter combination should be obtained to form the desired shape. As shown in Fig. 5, the coordinate system is established with the center of the plate as the original point O. The length and width of the plate are represented by l_1 and w_1, respectively. The width of the channel is defined as w_2. The distance between two channels is set to d_1. The distance between the outermost channel and the edge of the plate is indicated by d_2. Therefore, Eq. (1) can be used to determine the width of the channel and the distance between the channels. n_1 is the number of channels in the x-axis:

$$w_1 = 2d_2 + n_1 w_2 + (n_1 - 1)d_1 \tag{1}$$

As shown in the figure, the corner area is shown in red. Similarly, the straight channel and second-step structure are shown in blue and white, respectively. The length of the second-step structure is shown as l_2. l_3 is the length of the straight channel. The distance between second-step structures is called d_3. d_4 is the distance between the second-step structure and the corner area. Finally, the following formula can be obtained. n_2 is the number of second-step structures:

$$d_4 = \frac{l_3 - n_2 l_2 - (n_2 - 1)d_3}{2} \tag{2}$$

According to Eqs. (1) and (2), MATLAB is used to find the appropriate parameter combination. As shown in Fig. 6, the 3D surface diagram of Eq. (1) is shown. The relationship between the parameters can be visually displayed. As it can be seen from the figure, the number of channels (n_1) is easily affected by the width (w_2) and distance (d_1) of the channels. As the value of d_1 goes up, the value of n_1 gets smaller and smaller. In addition, the value of n_1 is decreased with the increase of parameter w_2. According to the MATLAB surface diagram, the appropriate width and distance of channels can be found.

The relationship between the parameters of Eq. (2) is shown in Fig. 7. As shown in the figure, the number of second-step structures (n_2) is directly affected by the length (l_2) and distance (d_3) of the second-step structures. When the length of second-step structure increases, the number of second-step structures is decreased. The number of second-step structures is also limited by the distance of second-step

Table 1 Parameters of micro-channel in different groups

No	Second-step structure length (mm)	Channel width (mm)	Height ratio of first to second step H_1:H_2 (mm)	Edge chamfer D_1:D_2 (mm)
1	5	1	0.30:0.30	0
2	6	1	0.30:0.30	0
3	7	1	0.30:0.30	0
4	7	1	0.30:0.30	0.125:0.30
5	7	1	0.30:0.30	0.25:0.30
6	7	1	0.30:0.30	0.375:0.30
7	7	1	0.30:0.30	0.50:0.30
8	7	1	0.35:0.25	0.50:0.30
9	7	1	0.40:0.20	0.50:0.30
10	7	1.1	0.30:0.30	0.55:0.30
11	7	1.2	0.30:0.30	0.60:0.30

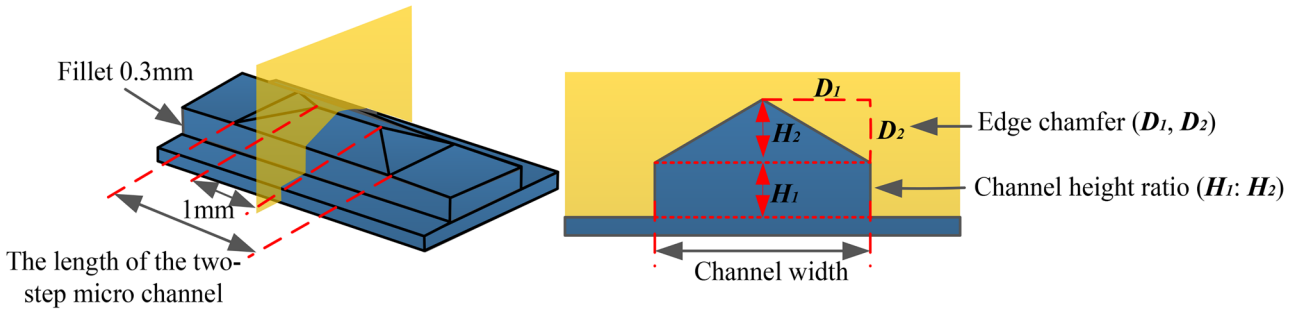

Fig. 4 Schematic diagram of geometrical parameters of two-step micro-channel

structures. Only when the parameters are appropriate, the suitable structural design can be obtained.

As shown in the figures above, when the size of the plate and the parameters of the two-step channel are changing, based on Eqs. (1) and (2) and MATLAB, the suitable parameter group can be found. The best design strategy can be provided by these parameters.

Moreover, based on the above parameters, the molds shown in Table 2 are also designed.

The assembly and meshing of molds, plates, and rubber pad in finite element simulations are shown in Fig. 8

In the rubber pad–forming process, the entire model is in a frame. Deformation is allowed only in the vertical direction because of frame. To simplify the simulation model, the role of the frame is replaced by additional constraints. The only free surface in the rubber pad is the one contact to the plate. The rest of all surfaces are limited by loads. Rigid mold is only allowed to move up in vertical direction to form the plate. With these loads, all deformation can be taken part into the forming of the micro-channel.

In this model, the mold is defined as a rigid part. Moreover, it is placed at the bottom of the entire model.

The plate is placed between the mold and the rubber pad. It is seen as a deformable part. SS304 was selected as the plate material. The friction between the plate and the mold is less than that between the plate and the rubber pad. The constant friction model is used in the analysis. The friction coefficients are entered as 0.1 and 0.2 [23, 24]. The thickness of the plate is selected as 0.1 mm. The density of plate is 7.833 g/cm^3. The Poisson's ratio and Young's modulus are 0.3 and 162.5 GPa, respectively. The yield stress and plastic strain of the plate satisfy the following relationship: $\sigma = 1421(0.047+\varepsilon)^{0.561}$.

The rubber pad is installed at the top of the model, which is also regarded as a deformable part. Polyurethane with hyperelasticity is selected as rubber pad material. The hardness of rubber is 70 Shore A. Because the nonlinear hyperelasticity and incompressible properties need to be defined on rubber material, the Mooney-Rivlin model is used. In addition, the parameters C10 and C01 in Mooney-Rivlin model were selected as 0.736 and 0.184 [3, 25].

As shown in Fig. 8, the rubber pad and plate are meshed. The total number of elements and nodes are 28,800 and 58,564, respectively. Mesh types of rubber pad and plate are C3D8RH (8-node linear brick, hybrid, constant pressure, reduced integration, hourglass control) and C3D8R (8-node linear brick, reduced integration, hourglass control), respectively. They are both in the same size 60 × 60 mm.

3 Results

In order to study the effects of different geometric parameters on forming results, not only the stress contours are displayed on the deformed plate, but also the shapes of micro-channels are shown.

As it is shown in Fig. 9, stress contours and forming results are shown. When the length of the second-step structure is different, the stresses on the plate are described by contours. When the length is 5 mm, the deformation between channels is insufficient. If the length is increasing

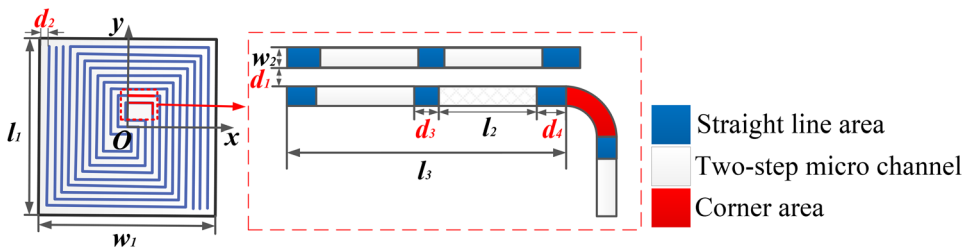

Fig. 5 Schematic diagram of partial plate parameters

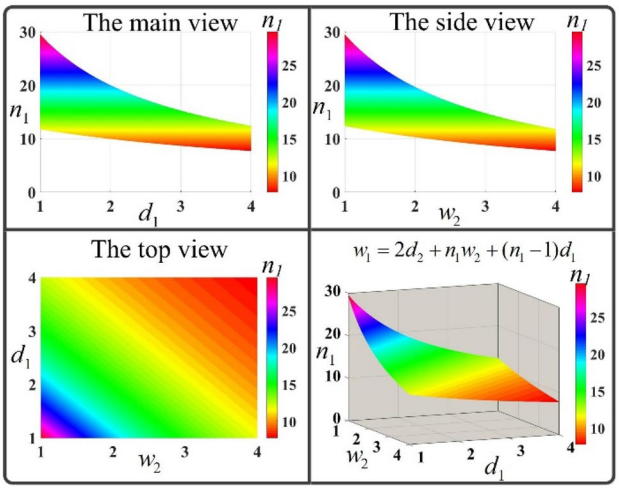

Fig. 6 Schematic diagram of MATLAB of Eq. (1) (d_1 the distance between two channels, w_2 the width of the channel, n_1 the number of channels)

from 5 to 7 mm, the stress shown on the plate is increasing based on these comprehensive reasons. The forming results of the plates also become better based on this changing. This can be explained that the flow of rubber will be less restricted when the second-step structure is long enough. The channel can be formed more accurately with larger stress.

However, as shown in Fig. 9, it is obvious that the ridge of two-step channel is not well formed. Actually, more stress is needed when the height of two-step channel is suddenly increased, due to the presence of the second-step structure. (The unit of the von Mises stress is Pa, and the unit of the displacement is mm.) Also, the shape of the second-step structure should be well adjusted to further

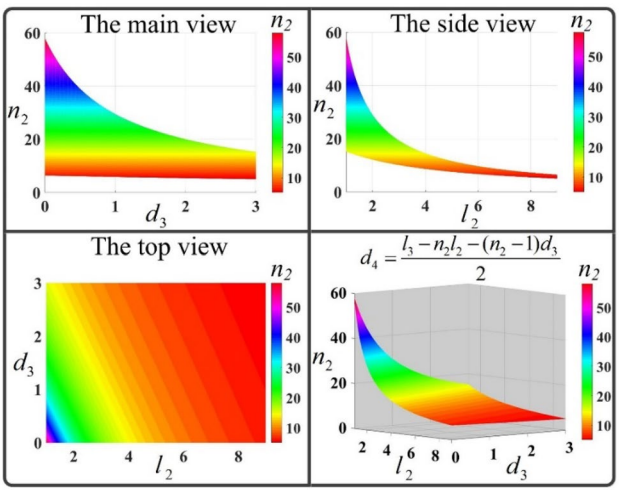

Fig. 7 Schematic diagram of MATLAB of Eq. (2) (d_3: the distance between second-step structures, l_2: the length of the second-step structure, n_2: the number of second-step structures)

Table 2 Parameters of micro-channel in different groups

No	The distance between the second-step structures d_3(mm)	No	The number of second-step structures
12	0	15	134
13	1	16	112
14	2	17	100

improve the formability. As shown in Fig. 10, different edge chamfers of the second-step structure are researched to improve this situation.

As it can be seen in Fig. 11, with the increase of edge chamfer (D_1, D_2), the forming result of the plate firstly become worse, and then a better result can be shown. When $D_1 \leq 0.25$ mm, the plate is suffered to a smaller stress, and the first-step channel is barely formed. When $D_1 > 0.25$ mm, the stress shown on the plate is increased, the first and second step channels are obviously formed, and the forming results are better. When edge chamfer D_1, D_2 are 0.5 mm and 0.3 mm, the shape of the top second-step structure is changed to straight line from rectangle. Since the edges of the second-step structure are accurately formed, the forming result can be better at this time.

As it is seen in Fig. 12, the channel height ratios of the first and second step are 0.3 mm:0.3 mm, 0.35 mm:0.25 mm, and 0.4 mm:0.2 mm, respectively. With the increase of the height ratio of the first and second step channel, the forming results are worse and worse. This may be explained by the flow of rubber is more restricted. As the height of the second-step structure is decreasing, the volume of the second-step structure will also be decreased. When the ratio is 0.3 mm:0.3 mm, the plate is suffered the maximum stress, and the forming result is the best.

The length, edge chamfer, and height ratio all have influence on the forming result, but the width of channel seems to play a most important role on the final result. This kind of influence has nothing to do with the forming ability of the plate, but it is the location of the interaction that most affects the result. As the width of the channel is increased, the distance between channels is decreased in this simulation. As shown in Fig. 13, when the channel width is increased from 1 to 1.2 mm, the forming results of the plates become worse and worse. This can be explained by the stress applied on the ridge of the channel. When the distance between channels is too small, the plate cannot be formed accurately and smoothly with less stress. As observed in the figure, the plates are well formed when the distance is 1.4 mm and 1.3 mm, respectively. At this point, the best formability of the second-step structure is found. Therefore, the distance between channels should be equal or greater than 1.3 mm.

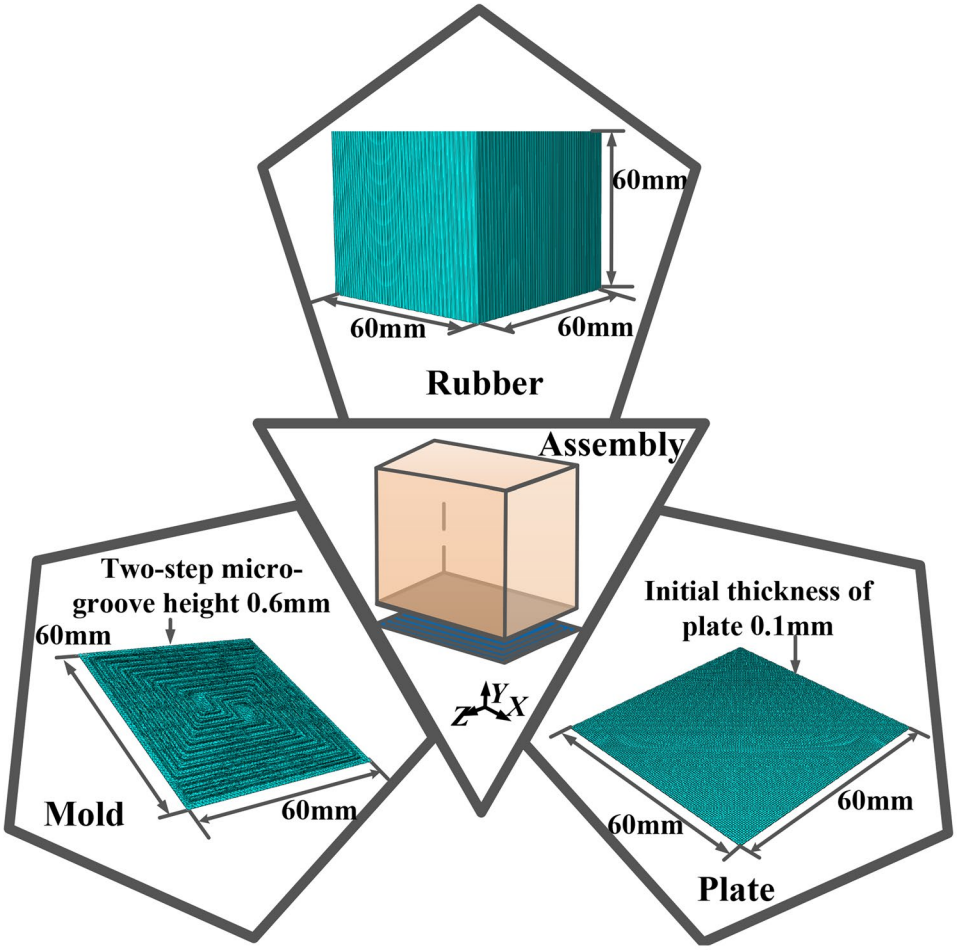

Fig. 8 Modeling and meshing as well as assembling of rubber pad forming simulation

The good forming results for the two-step micro channel were found according to the above simulations. The parameters with the suitable forming results were selected for the following study. Multiple two-step structures are designed in one micro-channel. As shown in Fig. 14, finite element simulation results were obtained when the distance between the second-step structures was 0 mm, 1 mm, and 2 mm, respectively. It can be observed that the stress applied on the channel is the same with each other. Moreover, the depths of micro-channel are the same as the design

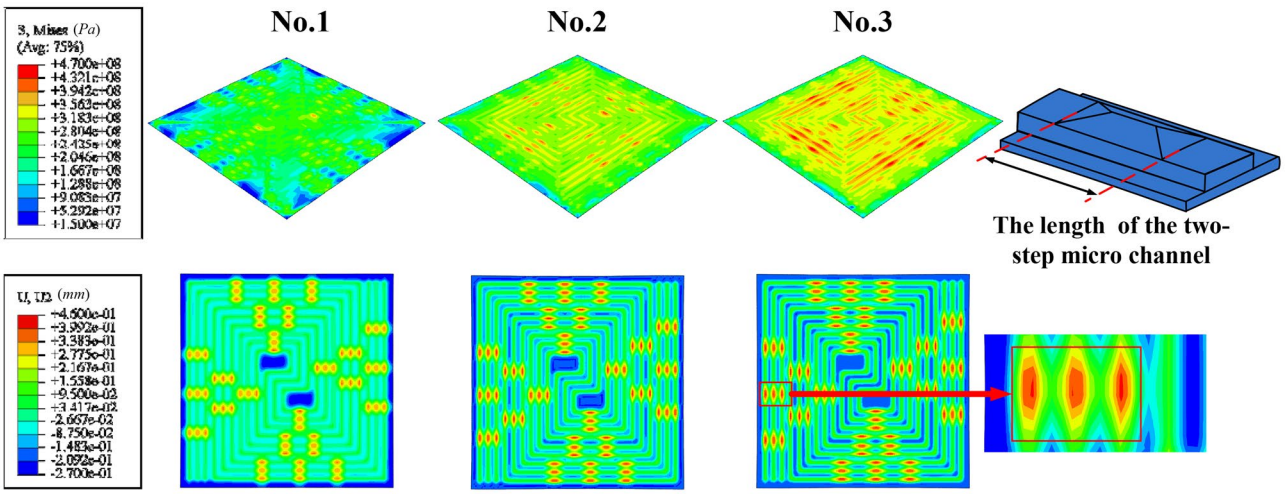

Fig. 9 Stress acting and displacement diagram of deformed plate by molds with different channel lengths (no. 1–no. 3)

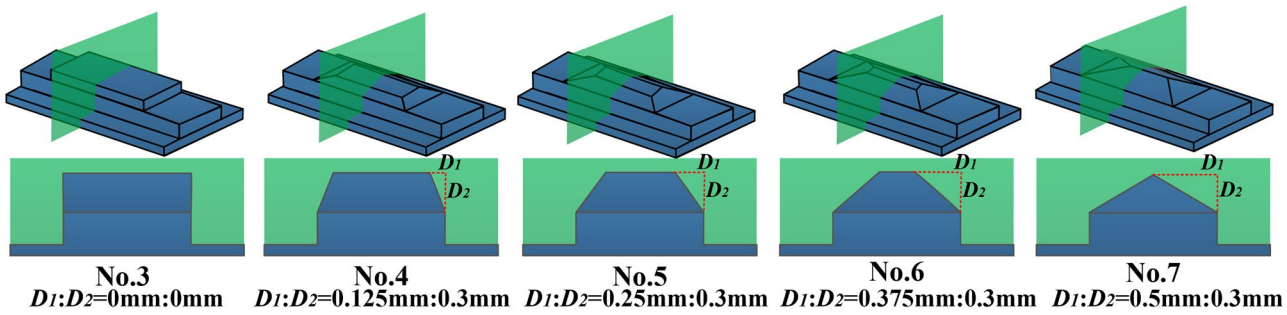

Fig. 10 Schematic diagram of edge chamfers of molds with D_1 and D_2 (no. 3–no. 7)

ones. Therefore, the distances between the second-step structures have a little influence on the forming results in nos.12, 13, and 14.

As shown in Fig. 15, the two-step channels with the largest number are inserted in the straight line areas. The lengths of the second-step structures are 7 mm, 8 mm, and 9 mm in no. 15, no. 16, and no. 17, respectively. According to Eq. (2), when parameter a is a constant value, parameters b and c are determined. It can be observed that the number of second-step structures is decreased as its length is increasing. When length of second step structure is 7 mm, there will be 134 ones. When the lengths are 8 mm and 9 mm, the quantities of this structure will be 112 and 100, respectively. As shown in the figure, the three plates are well formed. And it can be found that the straight line areas are all formed well. There are no obvious evidences to find a relationship between the number of second-step structures and formability.

In conclusion, the formable structure is obtained based on the following conditions met by each parameter.

1. The length of the second-step structure should be long enough (longer than 7 mm).
2. Edge chamfers should be as large as possible. The second-step structure can be minimized.
3. The height ratio of the first to second step should be 1:1.
4. The width of micro-channel should not be too small (greater than 1 mm is appropriate). And the distance between micro-channels should not be too small (greater than 1.3 mm is appropriate).
5. Even if the distance between the second-step structures is 0 mm, the formability of the entire plate will not be affected. Therefore, the second-step structure can be spaced as close as possible. Through this, the number of second-step structures can be increased.

4 Forming experiments

In order to further investigate the forming process of plate with two-step micro-channels, the rubber pad–forming experiment was also conducted. Based on the finite element simulation results, the parameters with the best forming results were selected [26]. Different molds are manufactured according to the channel parameters numbered no.7 and no.10.

As shown in Fig. 16, the experiment was carried out on a press machine with fixture. The stepping speed of the press machine is set as 0.5 mm/s. A frame is also used on the press machine to fix all the equipment. All deformations are limited in the vertical direction due to the frame. There are mold,

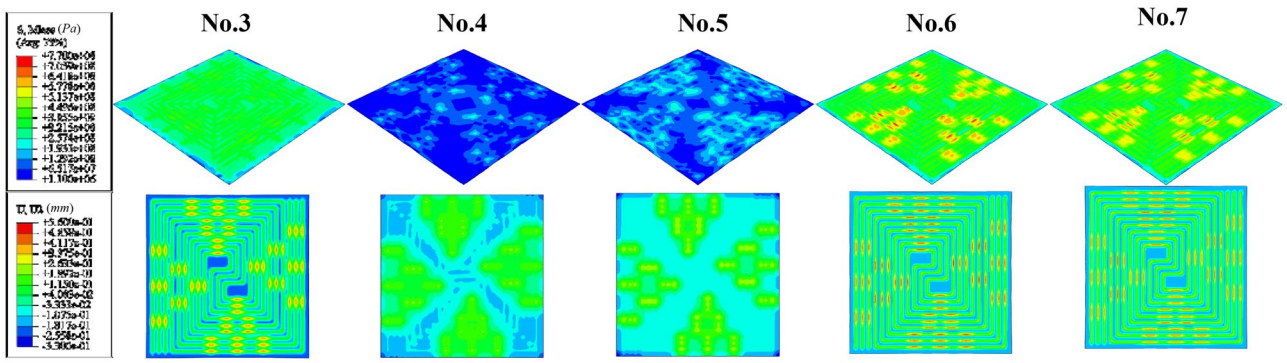

Fig. 11 Stress acting and displacement diagram of deformed plate by molds with different edge chamfers (no. 3–no. 7)

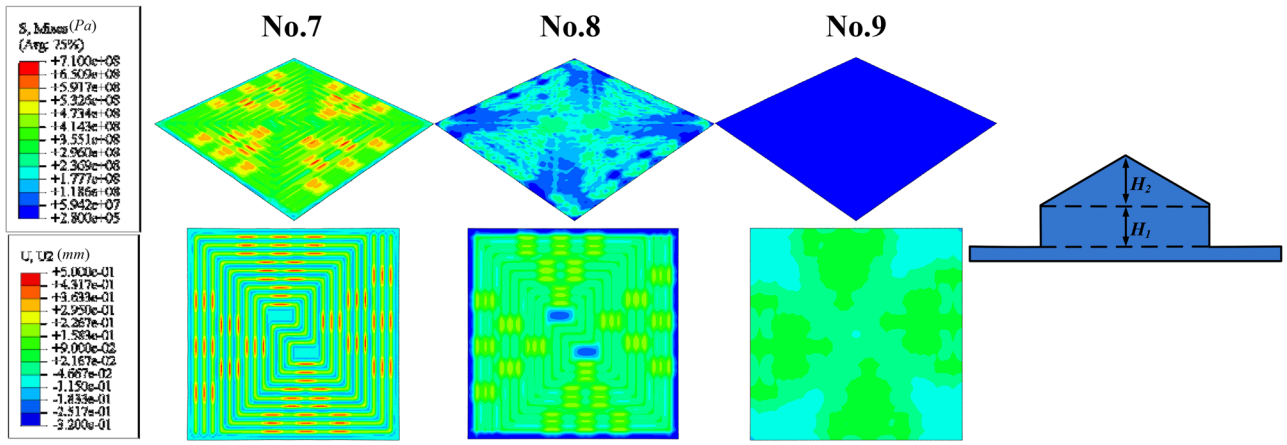

Fig. 12 Stress acting and displacement diagram of deformed plate by molds with different height ratios H_1:H_2 (no. 7–no. 9)

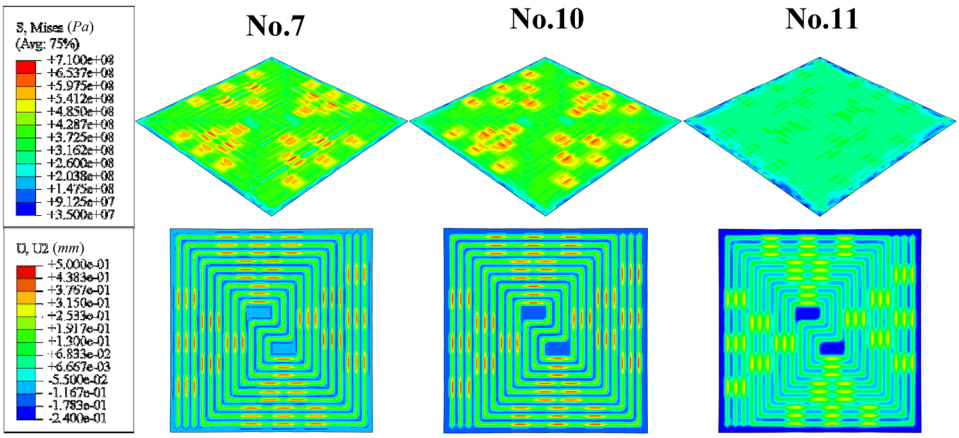

Fig. 13 Stress acting and displacement diagram of deformed plate by molds with different channel width (no. 7, no. 10, no. 11)

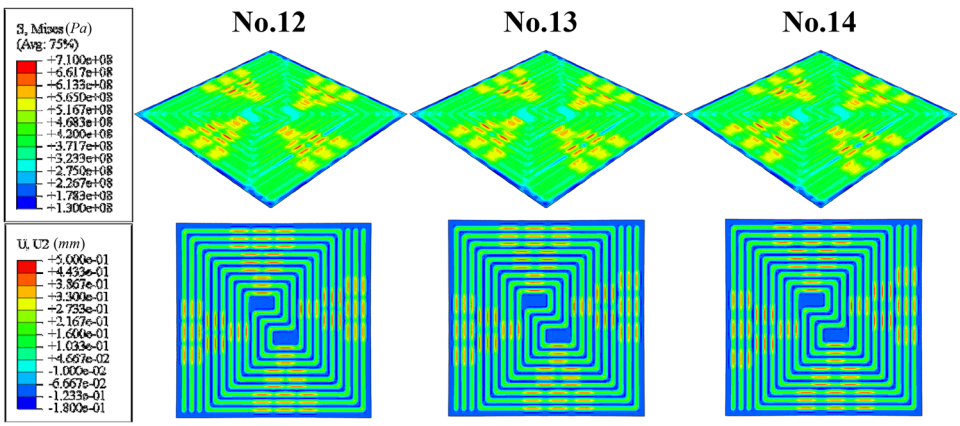

Fig. 14 Stress acting and displacement diagram of deformed plate by molds with different distance between the second-step structures (no. 12–no. 14)

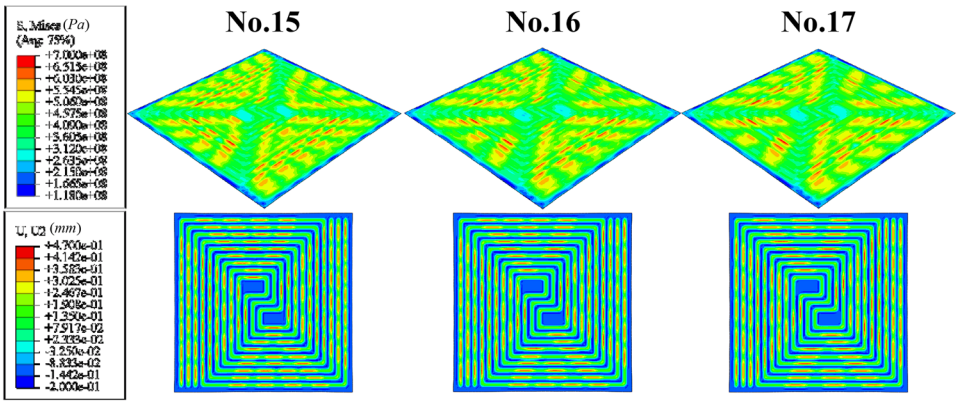

Fig. 15 Stress acting and displacement diagram of deformed plate by molds with different number of second-step structures (no. 15–no. 17)

Table 3 Chemical composition list of SS304

	C (%)	Si (%)	Mn (%)	P (%)	S (%)	Cr (%)	Ni (%)
SS304	≤0.08	≤0.1	≤0.2	≤0.045	≤0.03	18.00 ~ 20.00	8.00 ~ 10.50

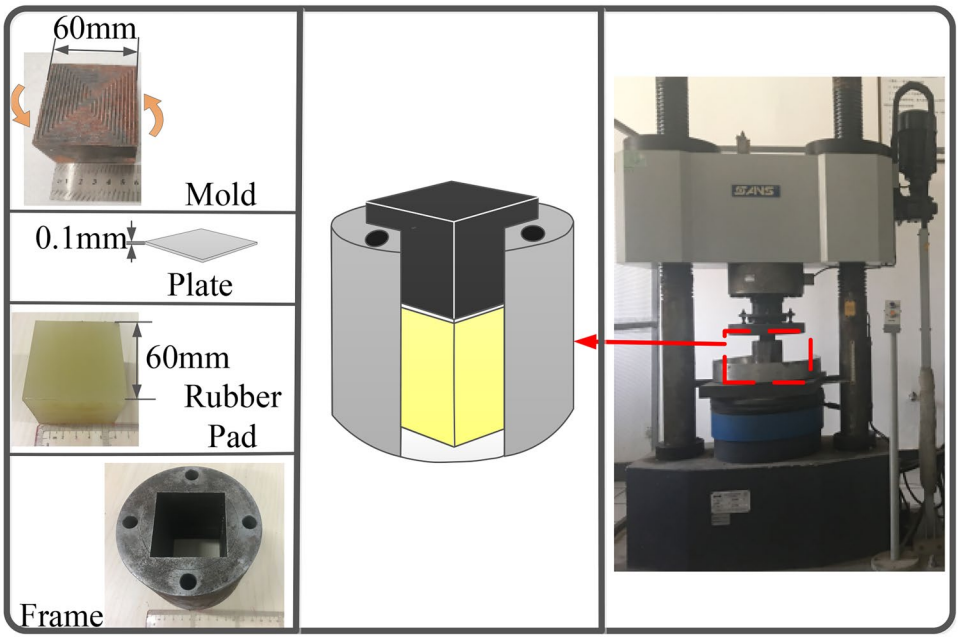

Fig. 16 Forming experiment

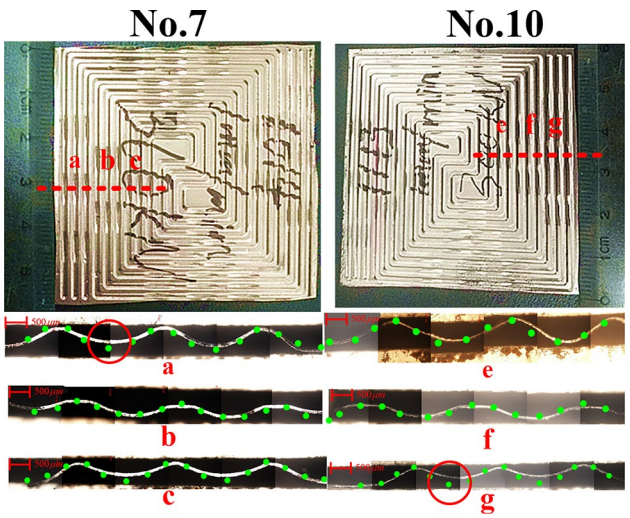

Fig. 17 Schematic diagram of forming results

plate, and rubber pad in the frame. They are all in the same size 60 mm × 60 mm. Their total height is slightly higher than that of the frame. So, when the press machine is turned on, the mold is pressed into the frame by the punch. Plate is also formed between the rubber pad and the mold. The mold is placed on top of these parts. It was placed upside down so that the channels can be formed on the plate as designed. As the material for the plates, SS304 has been annealed to improve its deformation capacities. Chemical composition of SS304 is shown in Table 3.

At the bottom, there is the rubber pad. Polyurethane is chosen as the material of rubber pad. Due to the limiting effect of the frame, the moving and deformation of the polyurethane are limited to the desired direction.

As shown in Fig. 17, after the pressing process, the plate was formed as it is designed. The channels of straight line and corner areas were easily seen on the plate. The

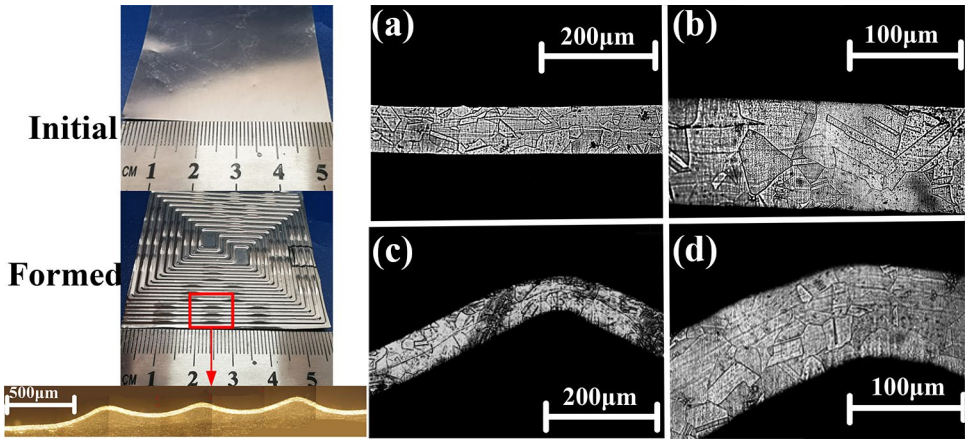

Fig. 18 Metallographic photographs of SS304 plate before and after deformation

second-step structure was obviously different from the first-step. As shown, the plates were cut along the red lines. The channels at the red lines in each plate were divided into three groups that are shown in both macroscopic and microscopic photos. In order to prove the results obtained based on the finite element method, the green lines representing the results of the finite element method are also shown in the figure. The results of the finite element method are in good agreement with the results of forming experiment. As shown in the figure, by comparing the results of finite element simulation and forming experiment, the height and width of the second-step and first-step channels are basically the same. However, there is a little error, circled in red, in the area between the second-step structures. This may be due to the springback of the plate after forming, which reduces the forming depth. It may also be caused by the secondary deformation of the section material during the cutting method.

Beyond that, as shown in the Fig. 18a, b, the metallographic photographs of the original SS304 plate are uniform distribution of austenite coarse grain structure, and the microstructure is uniform equiaxed grain. The metallographic photographs of SS304 after forming experiment are shown in the Fig. 18c, d. Compared with the microstructure before stamping, there will be plastic deformation of SS304, thus presenting different microstructure. The grains are elongated along the stamping direction. There are defects at grain boundaries, and dislocation density is increased.

5 Conclusion

1. Based on the finite element method, the punch and the rubber pad are combined to form the two-step channel. It can be found that when the main geometric parameters of the two-step micro-channel (channel width, length, height ratio, edge chamfer, and the spatial distribution of second-step structure) are different, the forming results can be obviously changed. The improper structure cannot be formed accurately in industrial production. Beyond that, the production cost will be increased. Therefore, it is very necessary to design the proper structure.
2. A new flow field design based on serpentine flow field and two-step channel is proposed. Based on finite element analysis and pressing experiment, the rubber pad–forming process can be used to form this flow field.
3. Through finite element analysis and forming experiment, a large width and distance of micro-channels, a large edge chamfer and length of second-step structure, a small distance of second-step structures, and a suitable first- and second-step height ratio are appropriate spatial distribution. Based on mathematical analysis and MATLAB, this structure design is still applicable in different plate sizes and channel parameters.

Author contribution Fei Teng and Hongyu Wang did the experiments and wrote the paper. Shengnan Shi and Jirui Li did the simulation and analysis. Juncai Sun, Jie Sun and Shunhu Zhang discussed.

Funding This study was funded by the National Natural Science Foundation of China No. 51905068, Doctor Start-up Foundation of Liaoning Province No.20180540098, Natural Science Foundation of Liaoning Province No.2020-HYLH-24, The open research fund from the state key laboratory of rolling and automation, Northeastern University No.2020RALKFKT012.

Availability of data and material The data and material are shown in the paper.

Declarations

Ethics approval Not applicable.

Consent to participate Not applicable.

Consent for publication This paper can be published.

Competing interests The authors declare no competing interests.

References

1. Browne DJ, Battikha E (1995) Optimization of aluminum sheet forming using a flexible die. Mater Process Tech 55(3–4):218–223
2. Belhassen L, Koubaa S, Wali M, Dammak F (2016) Numerical prediction of springback and ductile damage in rubber-pad forming process of aluminum sheet metal. Int J Mech Sci 117:218–226
3. Peng LF, Liu DA, Hua P, Lai XM, Ni J (2010) Fabrication of metallic bipolar plates for proton exchange membrane fuel cell by flexible forming process-numerical simulations and experiments. J Fuel Cell Sci Tech 73(3):299–302
4. Peng LF, Yi PY, Lai XM (2014) Design and manufacturing of stainless steel bipolar plates for proton exchange membrane fuel cells. Int J Hydrog Energy 39:21127–21153
5. Chen TC, Ye JM (2013) Fabrication of micro-channel arrays on thin stainless steel sheets for proton exchange membrane fuel cells using micro-stamping technology. Int J Adv Manuf Tech 64:1365–1372
6. Chen TC, Ye JM (2012) Analysis of stainless steel bipolar plates micro-stamping processes. Prz Elektrotechniczn 88(9B):121–126
7. Thiruvarudchelvan S (2002) The potential role of flexible tools in metal forming. J Mater Process Tech 122:293–300
8. Chen CH, Gau JT, Lee RS (2009) An Experimental and analytical study on the limit drawing ratio of stainless steel 304 foils for micro sheet forming. Mater Manuf Process 24(12):1256–1265
9. Wang HY, Teng F, Wei Z, Zhang PC, Sun JC, Ji SJ (2019) Simulation research about rubber pad forming of corner channel with convex or concave mould. J Mater Process Tech 40:94–104
10. Luo YH, Yuan L, Li JH, Wang JS (2015) Boundary layer drag reduction research hypotheses derived from bioinspired surface and recent advanced applications. Micron 79:59–73
11. Peker MF, Cora ON, Koc M (2011) Investigations on the variation of corrosion and contact resistance characteristics of metallic bipolar plates manufactured under long-run conditions. Int J Hydrog Energy 36:15427–15436
12. Mahabunphachai S, Koc M (2008) Fabrication of micro-channel arrays on thin metallic sheet using internal fluid pressure: investigations on size effects and development of design guidelines. J Power Sources 175:363–371
13. Wang GL, Niu D, Xie FQ, Wang Y, Zhao XL, Ding GF (2015) Experimental and numerical investigation of a microchannel heat sink (MCHS) with micro-scale ribs and grooves for chip cooling. Appl Therm Eng 85:61–70
14. Gau JT, Gu H, Liu XH, Huang KM, Lin BT (2015) Forming micro channels on aluminum foils by using flexible die forming process. J Manuf Process 19:102–111
15. Ghadikolaee HT, Elyasi M, Khatir FA, Hosseinzadeh M (2017) Experimental investigation of Fracture in rubber pad forming of bipolar plate's micro channels. Procedia Eng 207:1647–1652
16. Wang CT, Hu YC, Zheng PL (2010) Novel biometric flow slab design for improvement of PEMFC performance. Appl Energ 87(4):1366–1375
17. Juarez-Robles D, Hernandez-Guerrero A, Ramos-Alvarado B, Elizalde-Blancas F, Damian-Ascencio CE (2011) Multiple concentric spirals for the flow field of a proton exchange membrane fuel cell. J Power Sources 196(19):8019–8030
18. Yang YT, Tsai KT, Chen CK (2013) The effects of the PEM fuel cell performance with the waved flow channels. J Appl Math 5:1122–1203
19. Li WK, Zhang QL, Wang C, Yan XH, Shen SH, Xia GF, Zhu FJ, Zhang JL (2017) Experimental and numerical analysis of a three dimensional flow field for PEMFCs. Appl Energ 195:278–288
20. Wang HY, Wei Z, Teng F, Zhang PC, Sun JC, Ji SJ (2019) Numerical simulation and experiment research on forming of two-step channel based on rubber pad pressing. Int J Adv Manuf Tech 101:2175–2189
21. Waghmare GS, Arakerimath RR (2021) Prediction and optimization of multipoint dimple sheet forming of structural steel using Taguchi method. Mater Today: Proceedings 45(P6):5102–5107
22. Teng F, Wang HY, Sun JC, Kong XW, Sun J, Zhang SH (2020) Thickness analysis of complex two-step micro-groove on plate during rubber pad forming process. Proc Inst Mech Eng C J Mech Eng Sci 095440622093392
23. Liu YX, Hua L (2010) Fabrication of metallic bipolar plate for proton exchange membrane fuel cells by rubber pad forming. J Power Sources 195:3529–3535
24. Kolahdooz R, Asghari S, Rashid-Nadimi S, Amirfazli A (2016) Integration of finite element analysis and design of experiment for the investigation of critical factors in rubber pad forming of metallic bipolar plates for PEM fuel cells. Int J Hydrog Energy 42:1–15
25. Peng LF, Hu P, Lai XM, Mei DQ, Ni J (2009) Investigation of micro/meso sheet soft punch stamping process - simulation and experiments. Mater Des 30(3):783–790
26. Elyasi M, Khatir FA, Hosseinzadeh M (2017) Manufacturing metallic bipolar plate fuel cells through rubber pad forming process. Int J Adv Manuf Tech 89:3257–3269